



The larger crystals are mostly homogeneous though small inclusions of other phases are observed.

Mineral phase identifications were made by stoichiometry, guided by the P-T conditions of the experiments and referenced to published phase diagrams<sup>12</sup>. The silicate mineral phases are wadsleyite, majorite, Ca-majorite, ferropericlasite, and akimotoite. One grain of probable silicate perovskite was observed in each of the higher pressure runs (GN10 and GN11).

All metal grains in the samples are assemblages of two distinct phases. The textures range from lamellar to equigranular. These two phases are identifiable in BSE image based on contrast. The major phase across all three samples has an average composition of 83 wt% Fe and 14 wt% W, and the minor exsolved phase 70 wt% Fe and 27 wt% W. The remaining 3% are in Ni, Cr, and Mo. The exsolved phase comprises approximately 10% of the metal volume. Volume-averaged metal compositions were calculated for the partition coefficient computations of each sample.

Liquid metal/solid silicate partition coefficients ( $D_w$ ) were calculated for each silicate mineral phase from data for each sample run product. Liquid metal/liquid silicate coefficients were calculated for the identified melt regions of the two lower P runs, GN11 and GN13, labeled 'Melt' in Figure 2. Oxygen fugacities were determined from the compositions of ferropericlasite and coexisting metal, assuming ideal solutions. In Figure 2, all  $D_w$  were corrected to IW-2 fO<sub>2</sub> conditions to allow a more meaningful comparison of  $D_w$  values between phases and experiments and for comparison to published partitioning data. Other published data is shown from experiments conducted using a range of both silicate compositions and temperatures<sup>3,4,8,13,14,15,16</sup>.

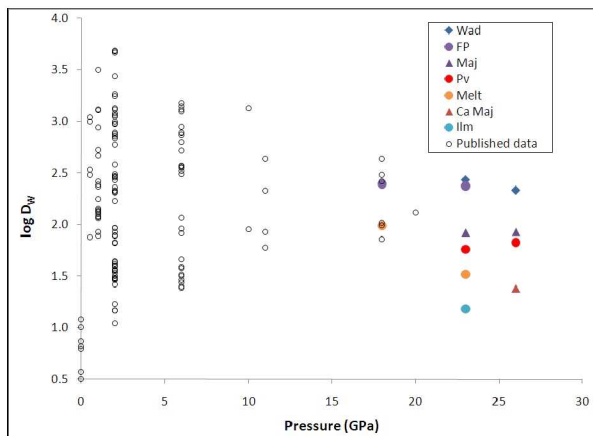


**Figure 2. Plot of log  $D_w$  vs. pressure for W.  $D_w$  values from our experiments are metal/mineral coefficients. Uncertainties on  $D_w$  range from 8% to 24%. Published data are shown for comparison.**

The present data suggest that the effect of higher-pressure (>10 GPa) on W partitioning is slight as shown by the nearly horizontal trend of the data. This is in accord with the interpretations of other authors<sup>5,8</sup>.

However, the current data set, including our experiments, still extend only to the mid-20 GPa range and the trajectory of W partitioning to pressures higher than approximately 26 GPa remains weakly constrained by experiments. It has been shown that predictions of high pressure behavior can fail to capture the actual behavior shown by experimental evidence, and therefore metal-silicate partitioning data at yet higher pressures will be an important addition to this discussion<sup>17,18</sup>.

**References:** [1] Righter, K. & Drake, M.J. (1996) *Icarus* 124, 513-529, [2] Halliday, A.N. (2003) *in* Davis (ed.) *Meteorites, Comets and Planets: Treatise on Geochemistry*, 509-557, [3] Walter, M.J. & Thibault, Y. (1995) *Science* 270, 1186-1189, [4] Hillgren, V.J., *et al.* (1996) *Geochim.* 60, 2257-2263, [5] Righter, K., *et al.*, (1997) *EPSL* 100, 115,134, [6] O'Neill H.St.C., *et al.*, (2008) *Chem Geol* 255, 346-359, [7] Ohtani, E., *et al.*, (1997) *Phys Earth Planet Int* 100, 97-114, [8] Cottrell, E., *et al.*, (2009) *EPSL* 281, 275-287, [9] Wade, J., & Wood, B.J. (2005) *EPSL* 236, 78-95, [10] Li, J., & Agee, C.B. (1996) *Nature* 381, 686-689, [11] Rudnick, R., *et al.*, (2004) *Lithos* 77, 609-637, [12] Gasparik, T. (2003) *in* *Phase diagrams for geoscientists: an atlas of the Earth's interior*, Springer-Verlag, Berlin, [13] Newsom, H.E. & Drake, M.J. (1982) *Geochim* 46, 2483-2489, [14] Jaeger, W.L. & Drake, M.J. (2000) *Geochim* 64, 3887-3895, [15] Righter, K. & Drake, M.J. (1999) *EPSL* 171, 383-399, [16] Shearer, C.K. & Righter, K. (2003) *GRL* 30, 1007-1-1007-4 [17] Tschauner *et al.*, (1999) *Nature* 398, 604-607, [18] Campbell *et al.*, (2009) *EPSL* 286, 556-564.